future pharmacology

MDPI

Communication

The Effect of Agave Bagasse Extract on Wound Healing in a Murine Model

Herminia López-Salazar [1,*], Elizabeth Negrete-León [2], Brenda Hildeliza Camacho-Díaz [1], Juan José Acevedo-Fernández [2], Sandra Victoria Ávila-Reyes [1] and Martha L. Arenas Ocampo [1,*]

[1] Centro de Desarrollo de Productos Bióticos, Instituto Politécnico Nacional, P.O. Box 24, Yautepec 62730, Morelos, Mexico; bhcamachod@gmail.com (B.H.C.-D.); sandra_victory@yahoo.com (S.V.Á.-R.)

[2] Laboratorio de Electrofisiología y Bioevaluación Farmacológica, Facultad de Medicina, Universidad Autónoma del Estado de Morelos (UAEM), Leñeros S/N, Los Volcanes, Cuernavaca 62350, Morelos, Mexico; elizabeth.negrete@uaem.mx (E.N.-L.) juan.acevedo@uaem.mx (J.J.A.-F.)

* Correspondence: herminia784@gmail.com (H.L.-S.); mlarenas@ipn.mx (M.L.A.O.)

Abstract: Background/Objectives: The development of bioproducts that can accelerate wound healing is a key focus in biomedicine, especially when these products are derived from sustainable by-products. This study investigates the wound-healing potential of an extract obtained from *Agave angustifolia* Haw bagasse (BagEE) using microwave extraction.Methods: HPLC-MS analysis was performed to identify the main compounds present in BagEE, revealing quercetin, isorhamnetin, diosgenin, hecogenin, manogenin, β-sitosterol glucoside, and β-sitosterol as tentative constituents. A murine excision wound model was employed to assess the efficacy of BagEE. The experimental group received a topical application of 8 mg of BagEE, while the control group was treated with water only. Wound closure, re-epithelialization, and collagen deposition were evaluated to determine the effects of BagEE on skin healing. Results: The BagEE-treated group exhibited significantly accelerated wound healing, achieving a 99.4% closure rate by day 13 compared to the control group's 92.8% closure rate on day 22. Additionally, wounds treated with BagEE displayed complete re-epithelialization and a well-organized skin structure. Conclusions: These findings suggest that BagEE promotes effective wound healing and shows promise as a topical agent for skin regeneration. Further studies are necessary to investigate its anti-inflammatory and wound-healing activities in both in vivo and in vitro settings.

Keywords: flavonoids; saponins; phytosterols; microwave

Academic Editor: Ali Zarrabi

Received: 30 December 2024
Revised: 12 January 2025
Accepted: 27 January 2025
Published: 5 February 2025

Citation: López-Salazar, H.; Negrete-León, E.; Camacho-Díaz, B.H.; Acevedo-Fernández, J.J.; Ávila-Reyes, S.V.; Ocampo, M.L.A. The Effect of Agave Bagasse Extract on Wound Healing in a Murine Model. *Future Pharmacol.* **2025**, *5*, 8. https://doi.org/10.3390/futurepharmacol5010008

1. Introduction

Maintaining the physiological balance of the human body relies heavily on the integrity of healthy skin. As the largest organ system, the skin plays a significant role in defending against mechanical damage, infections, fluid imbalances, and thermal regulation. It also provides flexibility in areas such as joints, while offering a more rigid structure in regions like the palms and soles to prevent excessive movement. Poor wound healing can be caused by a variety of factors, which may require medical treatment. Chronic diseases like diabetes and peripheral vascular disease can hinder the healing process, whereas acute injuries, such as degloving or severe burns, can cause a loss of skin function, making the body more vulnerable to infections, temperature imbalances, and dehydration [1].

A wound refers to a break or disturbance in the normal structure and function of tissues, which can involve the skin, mucous membranes, deeper tissues, or the surfaces of

internal organs. Wounds can manifest as incisions, lacerations, punctures, abrasions, or closed injuries such as hematomas, contusions, and crush injuries. When tissue integrity is compromised, a complex cascade of cellular events is triggered to repair the damage, ultimately leading to tissue reconstitution, resurfacing, and the restoration of tensile strength. The process of wound healing is complex and involves the synchronized collaboration of different tissues and cell types. This process requires careful control of cell movement, growth, matrix formation, remodeling, inflammation, and the formation of new blood vessels. While minor skin wounds can heal in a matter of days, larger injuries caused by trauma, severe illness, or major surgery may take several weeks to heal and frequently result in a fibrous scar that can impair the function of the affected tissue [2].

The process of wound healing occurs in three distinct and interrelated phases: inflammation, proliferation, and maturation. These phases are governed by the interactions of various growth factors, cytokines, and cell types, including keratinocytes, fibroblasts, and endothelial cells. During the inflammatory phase, important markers such as Nerve Growth Factor (NGF), Tumor Necrosis Factor-α (TNF-α), Interleukin-1, angiogenesis marker CD-31, and matrix metalloproteinases (MMPs) are essential. Keratinocytes aid in re-epithelialization, differentiation, and migration to cover the wound, while fibroblasts support tissue repair by promoting extracellular matrix proliferation. Endothelial cells contribute to the formation of new blood vessels, stimulated by signals from keratinocytes and fibroblasts [3].

Natural substances from herbal remedies have the potential to engage with various molecular targets. Due to their antioxidant, antimicrobial, and anti-inflammatory properties, these compounds have been employed in the pharmaceutical sector for wound treatment and tissue protection [4].

These plants are valued for their ability to modulate inflammation, enhance collagen synthesis, and promote tissue regeneration through angiogenesis. Among the most studied species are *Centella asiatica*, *Aloe vera*, and *Calendula officinalis*, each recognized for their bioactive compounds, including flavonoids, saponins, and terpenoids. These compounds contribute to their efficacy in wound repair and inspire further investigation into other plant genera with similar potential [5].

Centella asiatica, commonly known as gotu kola, is particularly celebrated for its efficacy in skin health and wound healing. This traditional herb is rich in bioactive compounds such as asiaticoside, madecassoside, asiatic acid, and madecassic acid, which synergistically enhance collagen deposition, regulate inflammatory pathways, and provide antioxidant protection. Recent studies have highlighted the benefits of its topical applications, demonstrating accelerated wound closure and improved recovery outcomes in complex cases like diabetic ulcers and burns [6].

Aloe vera, particularly *Aloe barbadensis*, has long been recognized for its medicinal benefits, especially in promoting the healing of burns, skin injuries, and ulcers. Studies have shown that Aloe vera gel accelerates wound healing, reduces edema, and alleviates pain. Research identified β-sitosterol—a compound found in *Aloe vera* gel—as the key factor responsible for its angiogenic effects, stimulating the formation of new blood vessels and promoting endothelial cell migration, which is essential for wound healing [7].

Calendula officinalis L., commonly known as calendula, is a medicinal plant from the Asteraceae family, widely used in products for wound care. Extracts from its flowers are rich in bioactive compounds, including saponins, flavonoids, and triterpenoids, which contribute to its antioxidant, anti-inflammatory, wound-healing, and antimicrobial properties. Notably, faradiol monoesters, a type of triterpenoid, are key to calendula's anti-inflammatory effects and promote fibroplasia and angiogenesis, aiding wound healing. Animal studies have shown that *Calendula officinalis* enhances collagen formation and

reduces epithelization time, particularly in skin loss and chronic wounds such as venous, pressure, and diabetic ulcers [8].

These properties have inspired the exploration of other plant species with similar potential, such as those in the Agave genus, which are abundant in bioactive metabolites with diverse pharmacological activities [9].

Agave is a valuable plant in Mexico, widely used across multiple sectors, including the production of beverages, food, biofuels, natural fibers, and secondary metabolites, contributing significantly to the economy. Species of Agave are abundant in a range of secondary metabolites, such as steroidal sapogenins, saponins, sterols, fructans, and flavonoids, among others. These metabolites demonstrate a variety of pharmacological activities, including immunomodulatory, cytotoxic, antiparasitic, and anti-inflammatory effects [10].

The manufacturing of tequila, mezcal, and agave fructans results in considerable waste, such as leaves, bagasse, and vinasse. Agave bagasse refers to the fibrous byproduct that remains after the agave hearts are cooked, crushed, and the sugars are extracted using water. This by-product represents a substantial waste component in agave-based industries and presents opportunities for sustainable valorization. Agave provides an abundant source of by-products with diverse potential for industrial applications, leading to the exploration of innovative processing methods aimed at sustainable revalorization of these residues [11].

To date, extracts derived from *Agave. angustifolia* Haw bagasse obtained through the fructan extraction process have not been evaluated for biological activity. Consequently, the objective of this study was to assess the in vivo wound-healing potential of an extract derived from agave bagasse. Moreover, a tentative identification of the major compounds in the extract was carried out to provide valuable insight into the bioactive components that might play a role in their wound-healing properties.

2. Materials and Methods

2.1. Plant Material

A five-year-old *A. angustifolia* plant, identified biologically, was harvested in Morelos, Mexico, at coordinates 18°49′33.3″ N and 99°06′21.98″ W, situated at an altitude above sea level. The bagasse from *A. angustifolia* was extracted using an aqueous method for fructans (Patent No. MX/E/2015/087857), a technique developed at the Center for Biotechnological Product Development (CEPROBI) in Yautepec, Morelos, Mexico. After extraction, the bagasse was collected and dried in an oven at 40 °C for 72 h to prevent microbial contamination. The dried material was then processed using a Gutstark mkz-Molin2000pla grinder, China, and passed through a 100-mesh sieve (0.150 mm mesh size), resulting in a final yield of 1000 g [12].

2.2. Extraction Technique

The extract used in this study was initially prepared in a previous work conducted by López-Salazar et al. in 2024 [12]; the extraction of secondary metabolites from *A. angustifolia* bagasse was carried out using microwave-assisted extraction (MAE). The extraction was carried out using a microwave oven (300 W at 2450 MHz) with CEM Discover® equipment, Matthews, NC, USA, under atmospheric conditions. A liquid-to-solid ratio of 20:1.6 mL/g was employed, with ethanol as the solvent. The process took place at a temperature range of 21–23 °C, with an extraction duration of 9 s.

2.3. HPLC–ESI–MS Analysis

The ethanolic extract of agave bagasse (BagEE) was analyzed through High-Performance Liquid Chromatography (HPLC) for its characterization. The analysis of BagEE was performed using HPLC-MS with a comprehensive set-up, which included

a CBM-20 system controller, two LC-20AD binary pumps, a DGY-20A5R degasser, an SIL-20AC autosampler, a CTO-20A column oven, an SPD-M20A UV-Vis photodiode detector, and an LCMS-2020 Mass Spectrometer with electrospray ionization (ESI). A reverse-phase RP-18 column (Lichrospher 100, 250 × 4 mm, RP-18, 5 µm) from Merck, (Darmstadt, Germany). was employed for separation, with an isocratic methanol: Mili-Q water (98:2) mobile phase. A 20 µL sample was injected, and the analysis was carried out at a flow rate of 1 mL/min over 40 min, with a column temperature maintained at 30 °C. The detection wavelength was set to 205 nm, and secondary metabolites were identified in the m/z range of 300–600. The capillary voltage was maintained at 4.5 kV, and nitrogen gas was used for nebulization [12].

The relative abundance of the major compounds was calculated using the following formula:

$$\% \text{ relative abundance} = \frac{\text{peak area of the compound}}{\text{total peak area of all compounds}} \times 100 \quad (1)$$

This approach allows for the quantification of each compound's contribution to the overall composition of the sample, facilitating a comparative analysis of the predominant components.

2.4. Animals

The study on wound healing was carried out using male CD1 mice (*Mus musculus*), aged between 2 and 3 months and weighing 30–40 g. These animals were sourced from the Animal Facility at the Universidad Autónoma del Estado de Morelos (UAEM). The experimental procedures received prior approval from the Institutional Animal Care and Use Committee of the Faculty of Medicine at UAEM (approval number: 006/2022; approval date: 12 August 2022) and adhered to the Technical Specifications for the Care and Use of Laboratory Animals (NOM-062-ZOO-1999).

2.4.1. Excision Wound Method

Sixteen mice were utilized for the study, separated into two groups of eight: one group served as the control and received distilled water, while the experimental group was treated with BagEE. The animals were acclimatized in the laboratory for seven days, housed individually with unrestricted access to food and water. For anesthesia, sodium pentobarbital (0.05 mg/g, Merck, CAS 57-33-0) was administered via intraperitoneal injection. The dorsal area was shaved, and a wound excision model was created by making a circular incision of 6 mm in diameter using a biopsy punch; this was considered as day 0.

The extract was in solid form, and for topical treatment, it was prepared using water as a vehicle. The formulation applied to the wounds in the experimental group had a concentration of 8 mg/mL, selected based on previous findings reported by Hernández-Valle et al. 2014 [13], where a similar concentration of an extract obtained from *A. angustifolia* demonstrated significant anti-inflammatory effects in a murine model. The control group wounds received 100 µL of distilled water, while those in the experimental group were treated topically with 100 µL of the BagEE solution.

The wound-healing process was monitored through photographs taken with an AmScope digital microscope camera, model Mu1000 (USB 2.0, DC 5 V/250 mA, P/N: US901000A, L/N: US2111011), manufactured in China. This camera was attached to a VELAB stereo zoom microscope, model VE-S5 (CA 110/240 V, 50/60 Hz), equipped with WF 10X/20 mm eyepieces, USA. This setup enabled high-resolution imaging and detailed observation of microscopic structures, ensuring precision in the visual data collected throughout the experimental procedures from the wound area, which was measured using Image J software 2.4.

2.4.2. Measurement of Wound Contraction

The wound contraction rate for each group was monitored on days 0, 1, 3, 6, 8, 10, 13, 15, 17, 20, and 22. The reduction in wound size was calculated as a percentage of the original wound area. The duration of epithelialization was assessed by counting the days until the eschar completely resolved, leaving no exposed wound area. Throughout the study, the percentage of wound contraction was recorded. This percentage was calculated using the following formula:

$$\% \text{ wound contraction} = \frac{\text{wound area day 0} - \text{wound area on day n}}{\text{wound area on day 0}} \times 100 \quad (2)$$

2.4.3. Histopathology Staining

Each group of animals was euthanized with an overdose of pentobarbital. After confirming death, the wounded areas were surgically excised, fixed in formalin, and embedded in paraffin following standard histotechnical procedures.

Histological analysis was performed on wound biopsies approximately 7 mm in diameter, encompassing the full skin thickness, and collected on day 22. The samples were preserved in formalin, embedded in paraffin blocks, and cut into 5 µm thick sections using a Leica RM 2125 RT microtome (Leica, Dallas, TX, USA). The tissue sections were then placed on glass slides and stained with hematoxylin and eosin for the assessment of the overall tissue structure. Collagen distribution, deposition, and fiber packing were further assessed using Masson's picropolychrome staining, which colored collagen fibers blue. All samples were examined under a Nikon Eclipse 80i (Tokyo, Japan) optical microscope.

For microscopic examination, the tissue sections were stained and observed at 400× magnification under a light microscope to assess the wound-healing areas.

2.5. Statistical Analysis

The data obtained were analyzed using one-way ANOVA, with Tukey's test applied to determine significant differences between groups ($p < 0.001$). Statistical analysis was carried out using SigmaPlot 11.0 software.

3. Results and Discussion

3.1. HPLC-MS Analysis

The HPLC-MS analysis of BagEE identified seven peaks, which are presented in Figure 1, arranged by their respective elution times. The compounds could be recognized based on their characteristic UV spectra and were identified using HPLC-MS data as well as by comparison with literature references.

The properties of each peak, such as retention time and theoretical and observed mass, along with the preliminary identification of the compounds, are presented in Table 1. The compounds identified in BagEE are as follows: quercetin detected at m/z 301 $[M + H]^+$ (experimental) with a retention time of 3.916 min in positive ionization mode (E^+); isorhamnetin detected at m/z 315 $[M + H]^+$ (experimental) with a retention time of 4.368 min in positive ionization mode (E^+); diosgenin detected at m/z 415 $[M - H]^-$ (experimental) with a retention time of 5.125 min in negative ionization mode (E^-); hecogenin detected at m/z 431 $[M - H]^-$ (experimental) with a retention time of 6.833 min in negative ionization mode (E^-); manogenin detected at m/z 446 $[M - H]^-$ (experimental) with a retention time of 8.876 min in negative ionization mode (E^-); β-sitosterol glucoside detected at m/z 575 $[M - H]^-$ (experimental) with a retention time of 9.771 min in negative ionization mode (E^-); β-sitosterol detected at m/z 414 $[M + H]^+$ (experimental) with a retention time of 23.037 min in positive ionization mode (E^+).

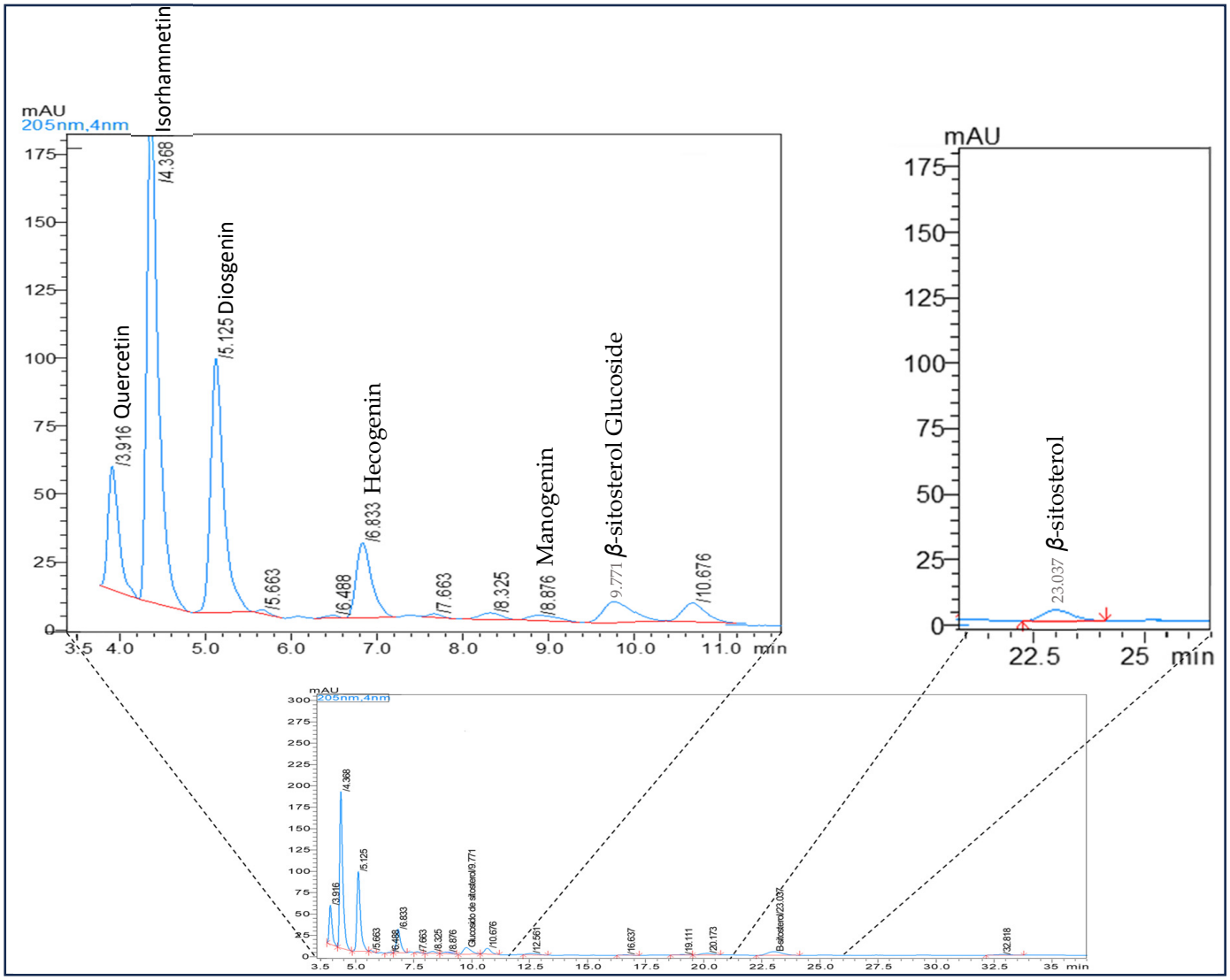

Figure 1. HPLC chromatogram of the ethanolic extract of agave bagasse (BagEE): Peaks corresponding to the major metabolites are labeled with their tentative identifications. The Y-axis represents the absorbance in milli-absorbance units (mAU), and the X-axis indicates the retention time (minutes). The identified compounds include quercetin (Rt 3.916 min), isorhamnetin (Rt 4.368 min), diosgenin (Rt 5.125 min), hecogenin (Rt 6.833 min), manogenin (Rt 8.876 min), β-sitosterol glucoside (Rt 9.771 min), and β-sitosterol (Rt 23.037 min), red arrows indicate the retention time range for β-sitosterol, marking both the initial and final points of its elution.

The compounds found in our study are consistent with those documented in the literature for the Agave genus. Research into the bioactive compounds responsible for the medicinal properties of agaves has grown substantially over time. The leaves and fibers, major byproducts from the production of tequila and mezcal, as well as from the textile industry, have been widely examined for their bioactive potential. Several studies have emphasized the value of agave processing waste as a rich source of secondary metabolites, such as phenols, flavonoids, phytosterols, and saponins [5].

For example, Morreeuw et al. [14] carried out a study aimed at identifying and quantifying the flavonoids found in the bagasse of *Agave lechuguilla*, also known as guishe. The researchers employed HPLC-UV-MS/MS techniques to analyze guishe samples from three different regions, investigating how various extraction solvents and storage conditions influenced the recovery of these bioactive compounds.

Table 1. Tentative identification of metabolites in the ethanolic extract of *Agave angustifolia* bagasse (BagEE) using HPLC-MS.

Compounds	Formula	*m*/*z* Theorical	*m*/*z* Experimental	PubChem ID	Retention Time (min)
Flavonoids					
• Quercetin	$C_{15}H_{10}O_7$	302.23	302	5280343	3.916
• Isorhamnetin	$C_{16}H_{12}O_7$	316.26	315	5281654	4.368
Saponins					
• Diosgenin	$C_{27}H_{42}O_3$	414.6	415	99474	5.125
• Hecogenin	$C_{27}H_{42}O_4$	430.6	431	91453	6.833
• Manogenin	$C_{27}H_{4205}$	447.31	446	-	8.876
Phytosterols					
• β-sitosterol Glucoside	$C_{35}H_{60}O_6$	576.8	575	5742590	9.771
• β-sitosterol	$C_{29}H_{50}O$	414.7	414	222284	23.037

The study provides details on the presence of isorhamnetin and quercetin in the samples. The findings reveal that quercetin and its glucoside derivatives, including isoquercetin, were present in substantial amounts in the ethanol extracts of guishe, particularly in samples from region 3, which exhibited greater flavonoid diversity. Region 3 refers to one of the geographical areas in Mexico selected for the collection of *A. lechuguilla* residues, characterized by a lower normalized difference vegetation index (NDVI) and an intermediate normalized difference water index (NDWI) compared to the other regions studied. Isorhamnetin and its glucosides were also identified, although their concentration varied depending on the region from which the samples were sourced [14].

They demonstrated that ethanol extracts exhibited a higher diversity and concentration of flavonoids compared to methanolic extracts, suggesting that ethanol is a more effective solvent for extracting compounds such as quercetin and isorhamnetin from guishe. The research evaluated the stability of the flavonoids under various storage conditions. The results showed that the bioactive compounds remained stable when the agro-residue was stored in an airtight container at room temperature and in the dark for nine months, which is significant for their potential industrial applications [14].

A different study by Morreeuw et al. [15] centered on extracting and characterizing bioactive compounds, with a particular emphasis on flavonoids. The researchers employed transcriptomic analysis to assess the flavonoid content in both processed and unprocessed leaf tissues of *A. lechuguilla*. By analyzing the first de novo transcriptome of *A. lechuguilla*, they identified genes involved in flavonoid biosynthesis, including those encoding enzymes and transcription factors.

The extraction process employed HPLC-MS/MS screening of alcoholic extracts, which demonstrated a significant expression of flavonoid biosynthesis genes in processed leaf tissues. This indicated an elevated presence of flavonoids and glycoside derivatives within the waste biomass. Focused HPLC-UV-MS analysis further quantified specific compounds, confirming the presence of isorhamnetin (1251.96 µg) and quercetin (15.57 µg) per gram of dry residue [15].

The study concluded that *A. lechuguilla* waste biomass has significant potential as a valuable source of bioactive flavonoids, with promising applications across various industries, including agriculture, food, cosmetics, and pharmaceuticals [15].

In a study utilizing the residues of *Agave sisalana*, an ethanolic extraction method was employed to isolate bioactive compounds, specifically the sapogenins hecogenin and tigogenin. The presence of these sapogenins in the ethanolic extract was confirmed through high-precision analytical methods, such as High-Performance Liquid Chromatography (HPLC) and Mass Spectrometry (MS) [16].

In a different investigation, the crude extract derived from *A. lechuguilla* by-products was assessed for its potential use as a feed supplement for juvenile *Litopenaeus vannamei* shrimp. The guishe (by-product of *A. lechuguilla* fiber extraction) was analyzed for its bioactive compounds, focusing on saponins and flavonols. The guishe underwent harvesting and was processed using mechanical pressing to produce the crude extract. The compounds were accurately detected and characterized through analytical identification performed using High-Performance Liquid Chromatography combined with Mass Spectrometry (HPLC-MS) [17].

The saponins identified in the analysis comprised diosgenin, esmilagenin, hecogenin, manogenin, tigogenin hexose, chlorogenin, and diosgenin diglucoside. Moreover, the extract also revealed the presence of the flavonol quercetin. These compounds highlight the nutritional and potential functional properties of the crude extract, which could be utilized as a feed additive [17].

Using microwave-assisted extraction (MAE), β-sitosterol (BSS) and β-sitosterol glucoside (BSSG) were effectively obtained from the bagasse of *A. angustifolia.* High-performance thin-layer chromatography (HPTLC) analysis quantified the yields, showing 103.6 mg/g for BSS and 61.6 mg/g for BSSG. Characterization of the compounds was further validated using FT-IR, HPLC-MS, and GC-MS [12].

Figure 2 illustrates the relative abundance (%) of the tentative major compounds identified in the BagEE using HPLC-MS. The analysis revealed that isorhamnetin was the predominant compound, accounting for 21.6% of the total composition, followed by diosgenin at 12.4% and quercetin at 4.9%. These results highlight the presence of bioactive flavonoids, saponins, and phytosterols as key components of the BagEE, demonstrating its potential as a source of valuable bioactive molecules.

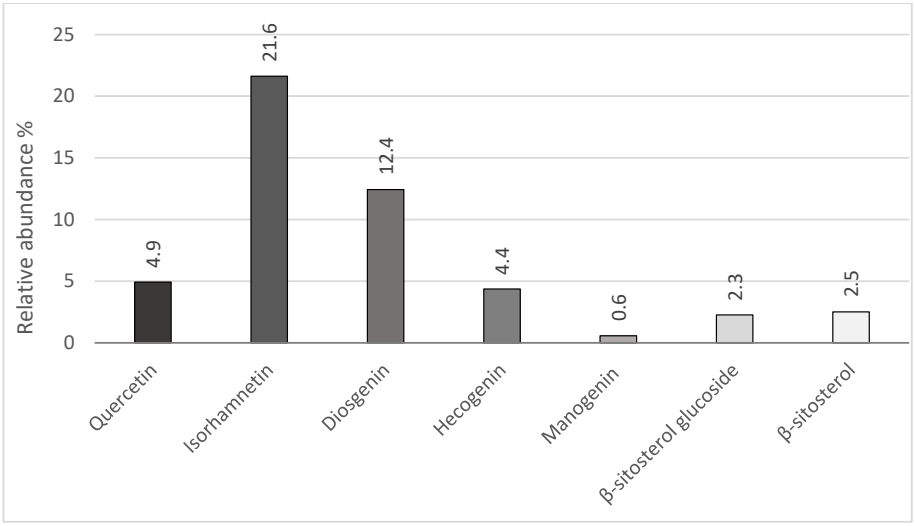

Figure 2. Relative abundance (%) of the tentative major compounds identified in the ethanolic extract of *Agave angustifolia* bagasse (BagEE) using HPLC-MS.

3.2. Wound Evaluation and Closure Percentage

A macroscopic assessment of the wound-healing process was conducted over a 22-day period. Figure 1 displays representative images of the wounds, illustrating the progressive reduction in the lesion area over time. By day 13, the group treated with BagEE achieved a

closure rate of 99.4%, which was notably higher compared to the control group's closure rate of 92.8%. The photographs show the wound closure progression in the control group, which received only water applications without treatment during the 22-day period. The control group exhibited slower wound closure compared to the BagEE-treated group, where the wound closed within 15 days following topical BagEE treatment, as shown in Figure 3.

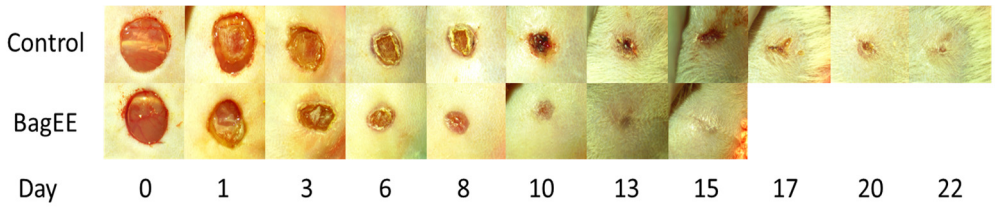

Figure 3. Photographs show the progression of wound closure over a 22-day period. Control group without treatment (water); BagEE: ethanolic extract of agave bagasse (n = 8 in each group).

Figure 4 illustrates the percentage of wound closure over the 22-day treatment period, comparing the control group and the BagEE-treated group. This figure provides a comprehensive view of the healing dynamics throughout the study, dividing the process into the three phases of healing: Phase I, Hemostasis/Inflammation (days 0–3); Phase II, Proliferative (days 4–8); and Phase III, Remodeling (days 9–22). From this analysis, it is evident that the application of BagEE resulted in a significantly higher percentage of wound closure during Phase I, corresponding to its anti-inflammatory activity, which accelerated the wound-healing process from the onset.

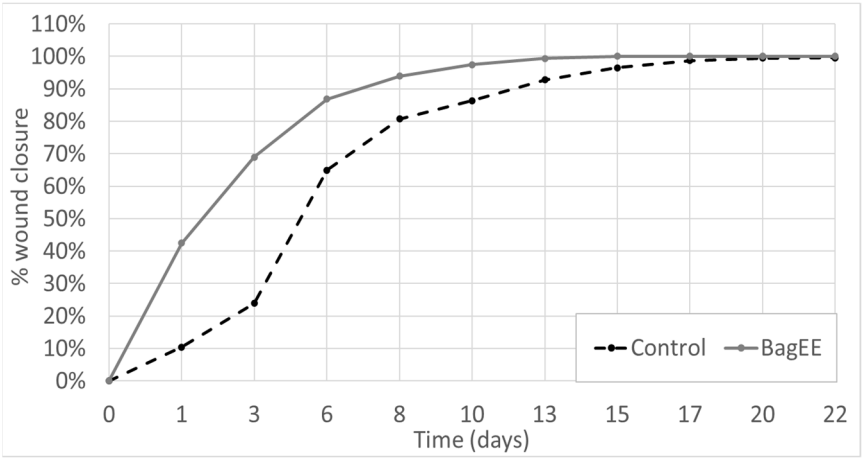

Figure 4. Dynamic evolution of wound closure. Temporal evolution of the wound area. Control group without treatment (water); BagEE: ethanolic extract of agave bagasse.

Additionally, Table 2 presents the average healing rates, highlighting temporal differences between the groups. It demonstrates that BagEE effectively accelerated wound healing, achieving a higher closure rate in the early stages of the process. Notably, BagEE reached its maximum healing rate on the first day of treatment, while the control group achieved its maximum rate only by day 6. This temporal advantage underscores the rapid action of BagEE in wound repair.

Table 2. Average wound closure speed.

Treatments	Days to Closing (Days)	Standard Deviation (Days)	Average Closing Speed (% per Day)	Maximum Speed
Control	19.286	±3.147	17.75	10.64% (on 6th day)
BagEE	13.250	±0.707	18.14	42.44% (on the 1st day)

The differences in the median values between the treatment groups are larger than what would be expected by random chance, indicating a statistically significant difference ($p \leq 001$) according to Tukey's test.

Wound healing typically progresses through a complicated, structured series of three interconnected stages: inflammation, proliferation, and remodeling. The inflammatory phase is characterized by vascular reactions that initiate exudation, coagulation, and hemostasis. In this phase, immune cells from blood vessels migrate to the wound area, releasing pro-inflammatory cytokines. Neutrophils and other immune cells generate reactive oxygen species (ROS), which are crucial for infection control but may harm adjacent tissues if produced in excessive amounts. In a typical healing response, immune cell presence and cytokine levels decrease within days, while keratinocytes, fibroblasts, and endothelial cells migrate to the site and begin secreting growth factors [18].

The proliferative phase then initiates, leading to epithelial formation to cover the wound surface and granulation tissue growth to fill the wound space. This tissue formation includes fibroblast proliferation, collagen and extracellular matrix (ECM) deposition, and new blood vessel formation, known as angiogenesis. Collagen synthesis also promotes wound contraction, reducing its size. As healing progresses, the provisional extracellular matrix (ECM) is gradually substituted by a mature scar, with type III collagen in granulation tissue being replaced by type I collagen, which is typical of normal dermis. This remodeling phase restores the tissue's structural integrity and function, a process governed by various growth factors and cytokines present at the wound site [19].

In our study, we observed that BagEE application significantly accelerated wound closure during Phase I, corresponding to the Inflammation Phase. This finding highlights BagEE's anti-inflammatory impact on the wound-healing process, as evidenced by photographs capturing the progression of wound closure.

The therapeutic potential of BagEE aligns with a broader understanding that natural products can enhance wound healing due to their medicinal properties. Numerous studies have emphasized the effectiveness of natural compounds in promoting wound healing, particularly those with anti-inflammatory, antioxidant, and antibacterial properties, and the ability to stimulate collagen synthesis. These positive effects are commonly linked to bioactive phytochemicals from various chemical groups, including alkaloids, essential oils, flavonoids, tannins, terpenoids, saponins, phenolic compounds, and phytosterols [12,20,21]

Each bioactive component appears to influence various aspects of the wound-healing process. For example, saponins are known to promote pro-collagen synthesis [19], while tannins and flavonoids exhibit potent antiseptic and antibacterial effects [16]. These phytochemicals can interact with multiple stages of wound repair and are easily absorbed by the skin's superficial layers [22].

The literature indicates that natural products with anti-inflammatory properties have been evaluated in wound-healing studies. Curcumin, the primary curcuminoid in *Curcuma longa* (turmeric), is a notable example of a natural product with significant wound-healing potential. Traditionally used in Indian herbal medicine for conditions such as rheumatism, diabetic ulcers, and respiratory issues, curcumin has shown anti-inflammatory, antioxidant, anticancer, antimutagenic, anticoagulant, and anti-infective properties. Its action mechanisms support multiple stages of wound healing, promoting faster tissue recovery. Research has documented curcumin's effectiveness in reducing inflammation and oxidative stress in skin wounds, with recent studies supporting its role in enhancing granulation tissue formation, collagen synthesis, tissue remodeling, and wound contraction [23].

In another study, the effects of topically applied curcumin on skin wound healing in diabetic rats were evaluated. Excisional wounds were induced on the skin of rats with streptozotocin-induced diabetes. The application of curcumin promoted wound contraction and reduced the levels of inflammatory cytokines and enzymes, such as tumor necrosis factor-alpha, interleukin (IL)-1β, and matrix metalloproteinase-9. Additionally, curcumin

treatment increased the levels of the anti-inflammatory cytokine IL-10 and antioxidant enzymes like superoxide dismutase, catalase, and glutathione peroxidase [24].

Flavonoids are among the metabolites involved in wound healing. Flavonoids have been widely researched for their ability to promote wound healing, which is mainly attributed to their anti-inflammatory, angiogenic, re-epithelialization, and antioxidant properties. These bioactive compounds influence the wound-healing process by regulating the expression of biomarkers linked to essential signaling pathways. Some of the key pathways affected include Wnt/β-catenin, Hippo, Transforming Growth Factor-beta (TGF-β), Hedgehog, c-Jun N-Terminal Kinase (JNK), NF-E2-related factor 2/antioxidant responsive element (Nrf2/ARE), Nuclear Factor Kappa B (NF-κB), MAPK/ERK, Ras/Raf/MEK/ERK, phosphatidylinositol 3-kinase (PI3K)/Akt, and Nitric Oxide (NO). These mechanisms highlight the therapeutic potential of flavonoids in facilitating tissue repair and regeneration [25].

A study focused on isorhamnetin, a flavonoid, demonstrated its potential to improve the therapeutic effects of mesenchymal stem cells derived from the umbilical cord (UC-MSCs) in the treatment of burn wounds. The results showed that isorhamnetin significantly improves the therapeutic potential of UC-MSCs by enhancing their anti-inflammatory, antioxidant, and tissue regeneration-promoting capacities. This compound boosted the expression of genes related to cell proliferation, angiogenesis, and wound healing, including vascular endothelial growth factor (VEGF) and interleukin-10 (IL-10), while simultaneously lowering inflammatory markers such as TNF-α. These findings position isorhamnetin as a key agent for improving cell therapies in severe wounds, emphasizing its modulatory role in skin repair and tissue regeneration processes [26].

In another study, researchers explored the combined use of chitosan and diosgenin, a steroidal saponin, for wound healing. They induced 6 mm diameter wounds on the backs of mice and treated them for 9 days with various substances, including chitosan and diosgenin. The results revealed that the chitosan–diosgenin combination (ChsDg) significantly reduced the wound area compared to other treatments [27].

Additionally, ChsDg maintained high levels of total glutathione (tGSH) in the wound tissues, suggesting its potential as an effective wound-healing agent. Diosgenin, a steroidal saponin, demonstrated substantial wound-healing potential through its anti-inflammatory, antioxidant, and pro-regenerative effects. The combination therapy showed superior efficacy compared to individual treatments, indicating a synergistic interaction. From a mechanistic perspective, diosgenin diminished the levels of inflammatory cytokines like TNF-α and IL-6, fostering a regulated inflammatory response essential for the healing process. It also enhanced antioxidant enzyme activity, including superoxide dismutase (SOD) and catalase (CAT), reducing oxidative stress at the wound site [27].

Diosgenin also enhanced the expression of angiogenic factors, such as vascular endothelial growth factor (VEGF), promoting the formation of new blood vessels critical for tissue regeneration. Diosgenin promoted fibroblast proliferation and extracellular matrix production, aiding re-epithelialization and enhancing tissue tensile strength. Experimentally, the chitosan–diosgenin combination accelerated wound closure, with histological analysis showing improved collagen deposition and reduced scar formation, demonstrating superior wound repair quality [27].

It has been shown that β-sitosterol glucoside, derived from *Trachelospermum jasminoides* (Apocynaceae), demonstrated anti-inflammatory properties in RAW 264.7 murine macrophages stimulated with lipopolysaccharides [28]. This evidence supports the potential role of phytosterols in modulating inflammatory responses and contributing to wound-healing processes.

Studies have linked BSS to enhanced wound healing, as demonstrated in research involving Aloe vera. This study showed that *Aloe vera* extracts containing BSS promoted

angiogenesis—a critical process in wound repair—on the chorioallantoic membrane (CAM) of chick embryos and in other in vivo models [7]. These findings suggest that BSS acts as a beneficial agent in tissue repair, implying that the extract from agave residue (BagEE) may also support wound healing through the bioactive effects of BSS.

The findings related to BSS and quercetin in the *Annona reticulata* leaf extract align with previous studies on BagEE, an extract derived from agave residues. Both studies highlight the potential of BSS as a key bioactive compound in promoting wound healing. While the *A. reticulata* study demonstrated accelerated wound closure in diabetic mice treated with its leaf extract [29], BagEE has also shown promise in enhancing wound repair processes, likely through mechanisms involving β-sitosterol's ability to stimulate angiogenesis and its anti-inflammatory activity. These parallels suggest that BSS could be a valuable agent in wound-healing applications, offering therapeutic benefits from various botanical sources and supporting its potential for broader pharmaceutical development in managing chronic wounds.

An important study to mention is one that investigated β-sitosterols and their proven effectiveness in promoting wound healing. Na^+/K^+-ATPase, beyond its role as a pump, is recognized for its signal transduction function, which plays a key role in cell growth regulation. The Na^+/K^+-ATPase/Src receptor complex is involved in multiple signaling pathways, including those that promote wound healing. In search of small molecular compounds to accelerate wound healing, the study focused on BSS, a natural compound with high inhibitory activity against Na^+/K^+-ATPase and non-cardiotoxic properties. A range of BSS derivatives was created, synthesized, and evaluated for their ability to inhibit Na^+/K^+-ATPase activity. [30].

Compounds 31, 47, and 49 showed enhanced Na^+/K^+-ATPase inhibitory activity compared to β-sitosterol (IC_{50} = 7.6 μM). Compound 31 contains an alkyl group and an electron-donating benzyl oxime ether substituent at position 3, contributing to an IC_{50} of 3.0 μM. Compound 47, with benzyl substitutions at positions 3 and 6 designed to maximize electron donation, achieved an IC_{50} of 3.4 μM. Compound 49, the most potent derivative, features a methyl group in the benzyl oxime ether fragment and optimized substituents, resulting in an IC_{50} of 2.2 μM.

Notably, compound 49 was observed to stimulate cell proliferation, migration, and the production of soluble collagen in L929 fibroblasts. In a rat model, compound 49 expedited the healing process of wounds. Additional research revealed that compound 49 activated proteins such as sarcoma (Src), protein kinase B (Akt), and extracellular signal-regulated kinase (ERK) in a concentration-dependent manner. The interaction of compound 49 with Na^+/K^+-ATPase was also explored, offering insights into the factors affecting its potency and selectivity. These results indicate that BSS derivative 49 is a potent Na^+/K^+-ATPase inhibitor and holds promise for enhancing wound healing [30].

Within the Agave genus, various studies have explored the bioactive properties that may be linked to wound healing. These investigations have highlighted the potential of Agave species to exhibit anti-inflammatory, antimicrobial, and regenerative effects, all of which are essential for effective wound repair. Below are some studies that evaluated certain compounds found in this research, demonstrating their relevance to the healing process [5].

A study was conducted to develop the alcoholic fraction of sisal (AFS) and characterize its sapogenins for potential phytotherapeutic applications. The research evaluated the cytotoxicity and anti-inflammatory effects of AFS both in vitro (through phagocytosis and hemolysis inhibition) and in vivo (assessing analgesic and anti-inflammatory activities). The study found that AFS contains hecogenin and tigogenin, with no cytotoxic effects. In vitro, AFS exhibited anti-inflammatory activity comparable to the positive control. In vivo, doses of 25 and 50 mg/kg AFS demonstrated significant anti-inflammatory effects, and a cream containing AFS showed similar activity. These effects are likely at-

tributed to the sapogenins present in AFS. Overall, the findings suggest that AFS possesses strong anti-inflammatory and analgesic properties, with potential for developing new treatments derived from sisal waste [16].

One example of a study investigating the biological activities of *Agave angustifolia* stem involved an acetonic extract obtained through maceration, which demonstrated anti-inflammatory effects. Further research identified 3-O-[6′-O-palmitoyl)-β-d-glucopyranosyl] sitosterol, stigmasterol, and β-sitosteryl glucoside as the compounds responsible for this activity. Both β-sitosterol (BSS) and its glucoside derivative, β-sitosterol β-d-glucoside (BSSG), are bioactive phytosterols known for their anti-inflammatory properties. Thus, the anti-inflammatory effects observed in *A. angustifolia* can be attributed to the presence of 3-O-[6′-O-palmitoyl)-β-d-glucopyranosyl] sitosterol [13].

Based on the studies cited above, it can be evidenced that BagEE plays an important role in several stages of the wound-healing process.

3.3. Histopathological Examination

In Figure 5B, corresponding to the BagEE-treated group, the early presence of granulation tissue, rapid re-epithelialization, and a well-healed dermis are confirmed, as shown in Figure 5D. These images show that wounds treated with BagEE exhibited enhanced granulation tissue formation, characterized by significant fibroblast proliferation and coverage by a thick, regenerated epithelial layer. In this group, the increased thickness of the epithelium suggests that the re-epithelialization process is further along, reflecting the active migration and proliferation of epithelial cells to efficiently cover the wound. This observation indicates that wound closure occurred more quickly in the BagEE-treated group than in the control group, as shown in Figure 5A,C. In the control group, a thinner epithelium is observed, suggesting that the healing process is still incomplete [31]. Figure 6A,B display panoramic views of the wound area, created by assembling multiple overlapping images to capture the complete skin wound landscape. To evaluate the morphological architecture of wound healing, tissue samples were collected on day 22 and stained with hematoxylin–eosin, revealing inflammatory cell infiltrate with a characteristic purplish-blue color, which aids in assessing scar structure and maturity [32].

As illustrated in Figure 6B, by day 22, the BagEE-treated group exhibited a fully re-epithelialized wound surface with a well-organized skin structure, including the presence of hair follicles and sebaceous glands, as shown in Figure 6D. In contrast, the control group shows no evidence of skin appendages, as shown in Figure 6C.

Additionally, the BagEE-treated group showed mature granulation tissue, characterized by high cellular density and reduced vascularization, whereas the control group retained immature granulation tissue. These findings suggest that BagEE treatment enhances wound healing by promoting the development of skin appendages and tissue maturation.

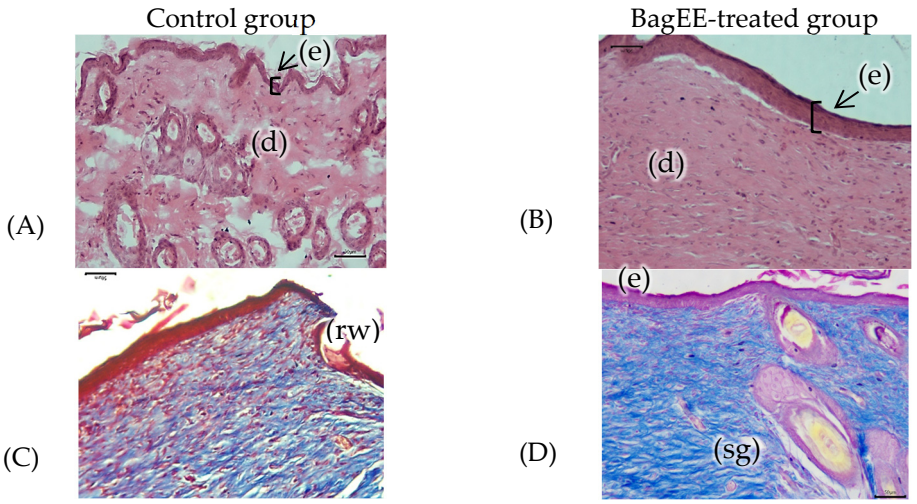

Figure 5. Photomicrographs (**A**,**B**) show the wound area of skin tissue after 22 days of treatment, stained with hematoxylin and eosin (H&E). (**A**) Control group without treatment (water-treated); (**B**) BagEE-treated group (ethanolic extract of agave bagasse). Magnification: 10×; scale bar: 50 µm. Photomicrographs (**C**,**D**) display the wound area of skin tissue after 22 days of treatment, stained with Masson's trichrome. (**C**) Control group without treatment (water); (**D**) BagEE-treated group (ethanolic extract of agave bagasse). Magnification: 10×; scale bar: 50 µm. Epidermis (e), dermis (d), residual wound (rw), and sebaceous gland (sg).

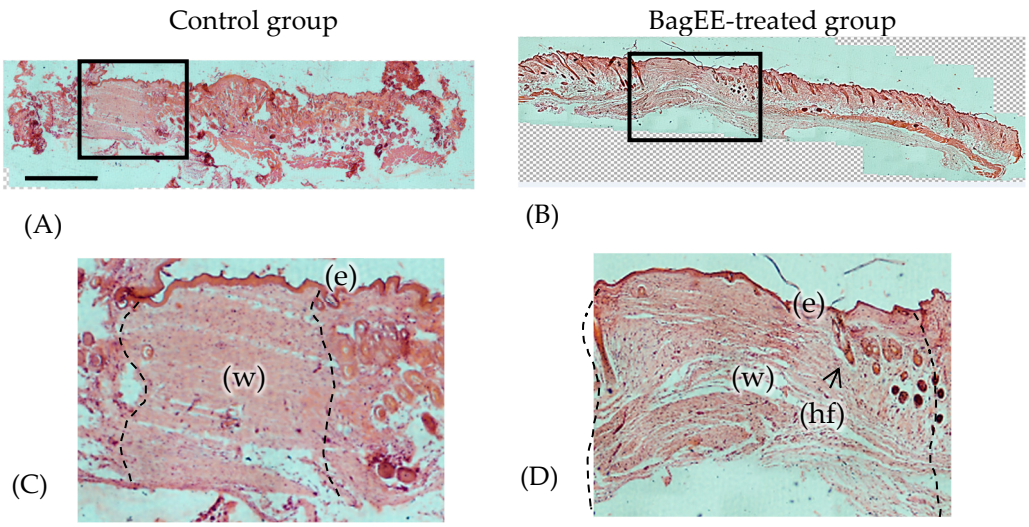

Figure 6. Photomicrographs (**A**,**B**) show the wound area of skin tissue after 22 days of treatment, stained with hematoxylin and eosin (H&E). A histological panoramic view of scar repair areas in each group highlights differences between treatments. Panel (**A**) shows the control group (water-treated), while Panel (**B**) represents the BagEE-treated group (ethanolic extract of agave bagasse). Notably, the BagEE-treated group exhibits complete re-epithelialization across the wound surface, contrasting with the control group, which shows immature epithelium. Scale bar: 1000 µm at higher magnification. The control group displays a thin layer of keratinized squamous epithelium without morphological signs of differentiation into cutaneous appendages. In contrast, the BagEE-treated group shows the presence of hair follicles, indicating advanced tissue maturation and regeneration. The dotted lines indicate granulation tissue. Epidermis (e), wound area (w), and hair follicles (hf). (**C**) higher magnification of (**A**), (**D**) higher magnification of (**B**).

Histomorphological evaluation of the wound collagen matrix architecture, shown in Figure 7, was conducted using Masson's trichrome staining, which highlights total collagen fiber content in blue. The BagEE-treated group, as shown in Figure 7B,D, displayed a more organized collagen matrix with thicker collagen fibers, while the control group

exhibited thinner, coarser fibers throughout the wound area, indicative of an earlier phase of epithelialization, as shown in Figure 7A,C.

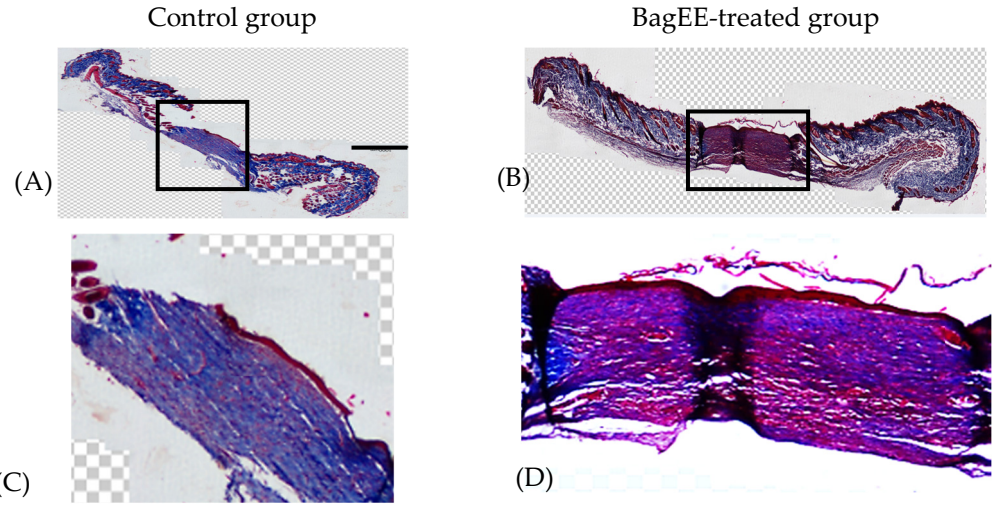

Figure 7. Photomicrographs (**A**,**B**) show the wound area of skin tissue after 22 days of treatment, stained by Masson's trichrome staining. A histological panoramic view of scar repair areas in each group. Scale bar: 1000 µm. Panel (**A**) shows the control group (water-treated), while Panel (**B**) represents the BagEE-treated group (ethanolic extract of agave bagasse). At higher magnification, details of the wound area are clearly visible. (**C**) higher magnification of (**A**), (**D**) higher magnification of (**B**).

In this group, the increased thickness of the epithelium suggests that the re-epithelialization process is further along, reflecting active migration and proliferation of epithelial cells to efficiently cover the wound. This observation indicates that wound closure occurred more quickly in the BagEE-treated group than in the control group [4].

4. Conclusions

In conclusion, it can be asserted that BagEE plays a crucial role in the wound-healing process, attributed to the bioactive compounds it contains, such as quercetin, isorhamnetin, diosgenin, hecogenin, manogenin, β-sitosterol glucoside, and β-sitosterol, which have demonstrated significant potential in promoting wound healing. However, further studies are essential to evaluate BagEE across various wound models and to thoroughly assess its long-term safety and efficacy. Standardized in vivo and in vitro studies, along with comparisons to current wound-healing treatments, are necessary to validate its therapeutic potential and explore its future clinical applications.

Author Contributions: Conceptualization, E.N.-L.; methodology, J.J.A.-F.; writing—original draft preparation, B.H.C.-D.; formal analysis, H.L.-S.; writing—review and editing, M.L.A.O.; visualization, S.V.Á.-R. All authors have read and agreed to the published version of the manuscript.

Funding: This study was funded by a postdoctoral fellowship provided by the Consejo Nacional de Humanidades, Ciencias y Tecnologías (CONACYT) in Mexico, CVU 551956.

Institutional Review Board Statement: The animal study protocol was authorized by the Institutional Animal Care Committee of the Faculty of Medicine at the Universidad Autónoma del Estado de Morelos (UAEM), with approval number 006/2022, granted on August 12, 2022. This study was conducted following the guidelines set by NOM-062-ZOO-1999, which outlines the technical specifications for the care and use of laboratory animals.

Informed Consent Statement: Not applicable.

Data Availability Statement: Dataset available on request from the authors.

Acknowledgments: We would like to express our sincere gratitude for the support received from CEPROBI-Instituto Politécnico Nacional and the Consejo Nacional de Humanidades, Ciencias y Tecnologías (CONAHCYT), Mexico, whose contributions were crucial in the preparation of this manuscript. Our heartfelt thanks also go to the Laboratory of Electrophysiology and Pharmacological Bioevaluation at the Faculty of Medicine, Universidad Autónoma del Estado de Morelos (UAEM), for their essential assistance and collaboration in this study. Furthermore, we extend our appreciation to the chromatography laboratory team at the Centro de Desarrollo de Productos Bióticos, Instituto Politécnico Nacional, with recognition to M.C. Alma Rosa López Laredo and M.C. Virginia Medina Pérez for their invaluable support and expertise throughout this research.

Conflicts of Interest: The authors declare no conflicts of interest.

References

1. Sorg, H.; Tilkorn, D.J.; Hager, S.; Hauser, J.; Mirastschijski, U. Skin wound healing: An update on the current knowledge and concepts. *Eur. Surg. Res.* **2017**, *58*, 81–94. [CrossRef] [PubMed]
2. Peña, O.A.; Martin, P. Cellular and molecular mechanisms of skin wound healing. *Nat. Rev. Mol. Cell Biol.* **2024**, *25*, 599–616. [CrossRef] [PubMed]
3. Tottoli, E.M.; Dorati, R.; Genta, I.; Chiesa, E.; Pisani, S.; Conti, B. Skin Wound Healing Process and New Emerging Technologies for Skin Wound Care and Regeneration. *Pharmaceutics* **2020**, *12*, 735. [CrossRef]
4. Ghosh, D.; Mondal, S.; Ramakrishna, K. A topical ointment formulation containing leaves extract of *Aegialitis rotundifolia* Roxb., accelerates excision, incision and burn wound healing in rats. *Wound Med.* **2019**, *26*, 100168. [CrossRef]
5. Ibrahim, N.I.; Wong, S.K.; Mohamed, I.N.; Mohamed, N.; Chin, K.-Y.; Ima-Nirwana, S.; Shuid, A.N. Wound Healing Properties of Selected Natural Products. *Int. J. Environ. Res. Public Health* **2018**, *15*, 2360. [CrossRef]
6. Witkowska, K.; Paczkowska-Walendowska, M.; Garbiec, E.; Cielecka-Piontek, J. Topical Application of Centella asiatica in Wound Healing: Recent Insights into Mechanisms and Clinical Efficacy. *Pharmaceutics* **2024**, *16*, 1252. [CrossRef] [PubMed]
7. Moon, E.J.; Lee, Y.M.; Lee, O.H.; Lee, M.J.; Lee, S.K.; Chung, M.H.; Kim, K.W. A novel angiogenic factor derived from Aloe vera gel: β-sitosterol, a plant sterol. *Angiogenesis* **1999**, *3*, 117–123. [CrossRef]
8. Giostri, G.S.; Novak, E.M.; Buzzi, M.; Guarita-Souza, L.C. Treatment of Acute Wounds in Hand with *Calendula officinalis* L.: A Randomized Trial. *Tissue Barriers* **2022**, *10*, 1994822. [CrossRef] [PubMed]
9. Bermúdez-Bazán, M.; Castillo-Herrera, G.A.; Urias-Silvas, J.E.; Escobedo-Reyes, A.; Estarrón-Espinosa, M. Hunting Bioactive Molecules from the *Agave* Genus: An Update on Extraction and Biological Potential. *Molecules* **2021**, *26*, 6789. [CrossRef]
10. Nava-Cruz, N.Y.; Medina-Morales, M.A.; Martinez, J.L.; Rodriguez, R.; Aguilar, C.N. *Agave* biotechnology: An overview. *Crit. Rev. Biotechnol.* **2014**, *35*, 546–559. [CrossRef] [PubMed]
11. Álvarez-Chávez, J.; Villamiel, M.; Santos-Zea, L.; Ramírez-Jiménez, A.K. Agave By-Products: An Overview of Their Nutraceutical Value, Current Applications, and Processing Methods. *Polysaccharides* **2021**, *2*, 720–743. [CrossRef]
12. López-Salazar, H.; Hildeliza Camacho-Díaz, B.; Arenas Ocampo, M.L.; Campos-Mendiola, R.; Martínez-Velarde, R.; López-Bonilla, A.; Ruperto Jiménez-Aparicio, A. Microwave-Assisted Extraction of β-Sitosterol: A by-Product from *Agave angustifolia* Haw Bagasse. *BioResources* **2024**, *19*, 568–581. [CrossRef]
13. Hernández-Valle, E.; Herrera-Ruiz, M.; Salgado, G.R.; Zamilpa, A.; Ocampo, M.L.A.; Aparicio, A.J.; Tortoriello, J.; Jiménez-Ferrer, E. Anti-Inflammatory Effect of 3-*O*-[(6′-*O*-Palmitoyl)-β-D-glucopyranosyl Sitosterol] from *Agave angustifolia* on Ear Edema in Mice. *Molecules* **2014**, *19*, 15624–15637. [CrossRef]
14. Morreeuw, Z.P.; Castillo-Quiroz, D.; Ríos-González, L.J.; Martínez-Rincón, R.; Estrada, N.; Melchor-Martínez, E.M.; Iqbal, H.M.N.; Parra-Saldívar, R.; Reyes, A.G. High Throughput Profiling of Flavonoid Abundance in *Agave lechuguilla* Residue-Valorizing under Explored Mexican Plant. *Plants* **2021**, *10*, 695. [CrossRef] [PubMed]
15. Morreeuw, Z.P.; Escobedo-Fregoso, C.; Ríos-González, L.J.; Castillo-Quiroz, D.; Reyes, A.G. Transcriptome-based metabolic profiling of flavonoids in *Agave lechuguilla* waste biomass. *Plant Sci.* **2021**, *305*, 110748. [CrossRef]
16. Fracasso, J.A.R.; Takahashi, M.E.; da Costa, L.T.S.; Barbosa, D.B.; Soares, B.A.; Pereira Martins, W.R.; Zoppe, N.A.; Marques, J.; Marques, M.P.M.; da Silva, A.M.; et al. Development of a Topical Cream from the Ethanolic of *Agave sisalana* Residues with Anti-Inflammatory and Analgesic Properties. *Cosmetics* **2024**, *11*, 180. [CrossRef]
17. Peña-Rodríguez, A.; Pelletier-Morreeuw, Z.; García-Luján, J.; Rodríguez-Jaramillo, M.D.C.; Guzmán-Villanueva, L.; Escobedo-Fregoso, C.; Reyes, A.G. Evaluation of *Agave lechuguilla* by-product crude extract as a feed additive for juvenile shrimp *Litopenaeus vannamei*. *Aquac. Res.* **2020**, *51*, 1336–1345. [CrossRef]
18. Kurahashi, T.; Fujii, J. Roles of Antioxidative Enzymes in Wound Healing. *J. Dev. Biol.* **2015**, *3*, 57–70. [CrossRef]
19. Zomer, H.D.; Trentin, A.G. Skin wound healing in humans and mice: Challenges in translational research. *J. Dermatol. Sci.* **2018**, *90*, 3–12. [CrossRef]

20. Thakur, R.; Jain, N.; Pathak, R.; Sandhu, S.S. Practices in Wound Healing Studies of Plants. *Evid.-Based Complement. Altern. Med.* **2011**, *2011*, 438056. [CrossRef]
21. Lin, T.-K.; Zhong, L.; Santiago, J.L. Anti-Inflammatory and Skin Barrier Repair Effects of Topical Application of Some Plant Oils. *Int. J. Mol. Sci.* **2018**, *19*, 70. [CrossRef]
22. Tsala, D.E.; Amadou, D.; Habtemariam, S. Natural wound healing and bioactive natural products. *Phytopharmacology* **2013**, *4*, 532–560.
23. Akbik, D.; Ghadiri, M.; Chrzanowski, W.; Rohanizadeh, R. Curcumin as a wound healing agent. *Life Sci.* **2014**, *116*, 1–7. [CrossRef]
24. Kant, V.; Gopal, A.; Pathak, N.; Kumar, P.; Tandan, S.K.; Kumar, D. Antioxidant and anti-inflammatory potential of curcumin accelerated the cutaneous wound healing in streptozotocin-induced diabetic rats. *Int. Immunopharmacol.* **2014**, *20*, 322–330. [CrossRef] [PubMed]
25. Zulkefli, N.; Che Zahari, C.N.M.; Sayuti, N.H.; Kamarudin, A.A.; Saad, N.; Hamezah, H.S.; Bunawan, H.; Baharum, S.N.; Mediani, A.; Ahmed, Q.U.; et al. Flavonoids as Potential Wound-Healing Molecules: Emphasis on Pathways Perspective. *Int. J. Mol. Sci.* **2023**, *24*, 4607. [CrossRef] [PubMed]
26. Aslam, S.; Khan, I.; Jameel, F.; Zaidi, M.B.; Salim, A. Umbilical cord-derived mesenchymal stem cells preconditioned with isorhamnetin: Potential therapy for burn wounds. *World J. Stem Cells* **2020**, *12*, 1652. [CrossRef]
27. Petrov, L.; Stoilova, O.; Pramatarov, G.; Kanzova, H.; Tsvetanova, E.; Andreeva, M.; Georgieva, A.; Atanasova, D.; Philipov, S.; Alexandrova, A. Effect of Chitosan-Diosgenin Combination on Wound Healing. *Int. J. Mol. Sci.* **2023**, *24*, 5049. [CrossRef] [PubMed]
28. Choi, J.N.; Choi, Y.H.; Lee, J.M.; Noh, I.C.; Park, J.W.; Choi, W.S.; Choi, J.H. Anti-inflammatory effects of β-sitosterol-β-D-glucoside from *Trachelospermum jasminoides* (Apocynaceae) in lipopolysaccharide-stimulated RAW 264.7 murine macrophages. *Nat. Prod. Res.* **2012**, *26*, 2340–2343. [CrossRef] [PubMed]
29. Mazumdar, S.; Ghosh, A.K.; Dinda, M.; Das, A.K.; Das, S.; Jana, K.; Karmakar, P. Evaluation of wound healing activity of ethanol extract of *Annona reticulata* L. leaf both in vitro and in diabetic mice model. *J. Tradit. Complement. Med.* **2021**, *11*, 27–37. [CrossRef]
30. Cui, S.; Jiang, H.; Chen, L.; Xu, J.; Sun, W.; Sun, H.; Qu, W. Design, synthesis and evaluation of wound healing activity for β-sitosterols derivatives as potent Na+/K+-ATPase inhibitors. *Bioorg. Chem.* **2020**, *98*, 103150. [CrossRef]
31. Rippa, A.L.; Kalabusheva, E.P.; Vorotelyak, E.A. Regeneration of Dermis: Scarring and Cells Involved. *Cells* **2019**, *8*, 607. [CrossRef]
32. Pérez-Contreras, C.V.; Alvarado-Flores, J.; Orona-Ortiz, A.; Balderas-López, J.L.; Salgado, R.M.; Zacaula-Juárez, N.; Navarrete, A. Wound healing activity of the hydroalcoholic extract and the main metabolites of *Amphipterygium adstringens* (cuachalalate) in a rat excision model. *J. Ethnopharmacol.* **2020**, *293*, 115313. [CrossRef] [PubMed]